

SCIENTIFIC REPORTS

OPEN

Selective Audiovisual Semantic Integration Enabled by Feature-Selective Attention

Received: 28 May 2015
Accepted: 30 November 2015
Published: 13 January 2016

Yuanqing Li¹, Jinyi Long¹, Biao Huang², Tianyou Yu³, Wei Wu⁴, Peijun Li⁵, Fang Fang & Pei Sun

An audiovisual object may contain multiple semantic features, such as the gender and emotional features of the speaker. Feature-selective attention and audiovisual semantic integration are two brain functions involved in the recognition of audiovisual objects. Humans often selectively attend to one or several features while ignoring the other features of an audiovisual object. Meanwhile, the human brain integrates semantic information from the visual and auditory modalities. However, how these two brain functions correlate with each other remains to be elucidated. In this functional magnetic resonance imaging (fMRI) study, we explored the neural mechanism by which feature-selective attention modulates audiovisual semantic integration. During the fMRI experiment, the subjects were presented with visual-only, auditory-only, or audiovisual dynamical facial stimuli and performed several feature-selective attention tasks. Our results revealed that a distribution of areas, including heteromodal areas and brain areas encoding attended features, may be involved in audiovisual semantic integration. Through feature-selective attention, the human brain may selectively integrate audiovisual semantic information from attended features by enhancing functional connectivity and thus regulating

An audiovisual object in the real world contains multiple semantic features, such as the gender and emotional features of a speaker's face and voice. During the recognition of an audiovisual object, the human brain integrates the semantic information from the features obtained by the visual and the auditory modalities, i.e., audiovisual semantic integration may occur in the brain. Audiovisual integration facilitates rapid, object and object-specific perception and recognition¹⁻³. Comparison of visual-only and audio-only stimuli has revealed that long-term audiovisual integration depends on the temporal relationship of stimuli alone in the perception

of audiovisual objects, such as low-level audiovisual integration, in which the semantic information of the audiovisual stimuli is not involved, and high-level audiovisual semantic integration⁴, the audiovisual semantic integration has been limited compared with the audiovisual integration. In particular, the mechanism underlying the modulation of audiovisual semantic integration in the brain by feature-selective attention has not been elucidated.

Previous studies have mainly focused on cross-modal attention and explored how cross-modal attention modulates audiovisual integration and attention during non-semantic visual-only, audio-only and audiovisual stimuli, an analysis of event-related potential (ERP) indicated that the effect of audiovisual integration requires the audiovisual object be fully attended. The audiovisual integration of motion information in the

¹Center for Brain Computer Interfaces and Brain Information Processing, South China University of Technology, Guangzhou, 510640, China. ²Department of Radiology, Guangdong General Hospital, Guangzhou, 510080, China. ³Department of Psychology and Key Laboratory of Machine Perception (Ministry of Education), Peking University, Beijing 100871, China. ⁴Department of Psychology, School of Social Sciences, Tsinghua University, Beijing, 100084, China. ⁵Guangzhou Key Laboratory of Brain Computer Interaction and Applications, Guangzhou 510640, China. Correspondence and requests for materials should be addressed to Y.L. (email: auyqli@scut.edu.cn)

a, precuneus, which helps in the perceptual and perceptual-motor integration of the visual information. The functional connectivity between the precuneus and the medial prefrontal cortex is important for the integration of the visual information and the generation of the perceptual-motor response. The functional connectivity between the precuneus and the medial prefrontal cortex is important for the integration of the visual information and the generation of the perceptual-motor response. The functional connectivity between the precuneus and the medial prefrontal cortex is important for the integration of the visual information and the generation of the perceptual-motor response.

In a single (visual) modality, the perceptual-motor integration of the visual information leads to the perceptual-motor response. The perceptual-motor integration of the visual information leads to the perceptual-motor response. The perceptual-motor integration of the visual information leads to the perceptual-motor response. The perceptual-motor integration of the visual information leads to the perceptual-motor response. The perceptual-motor integration of the visual information leads to the perceptual-motor response.

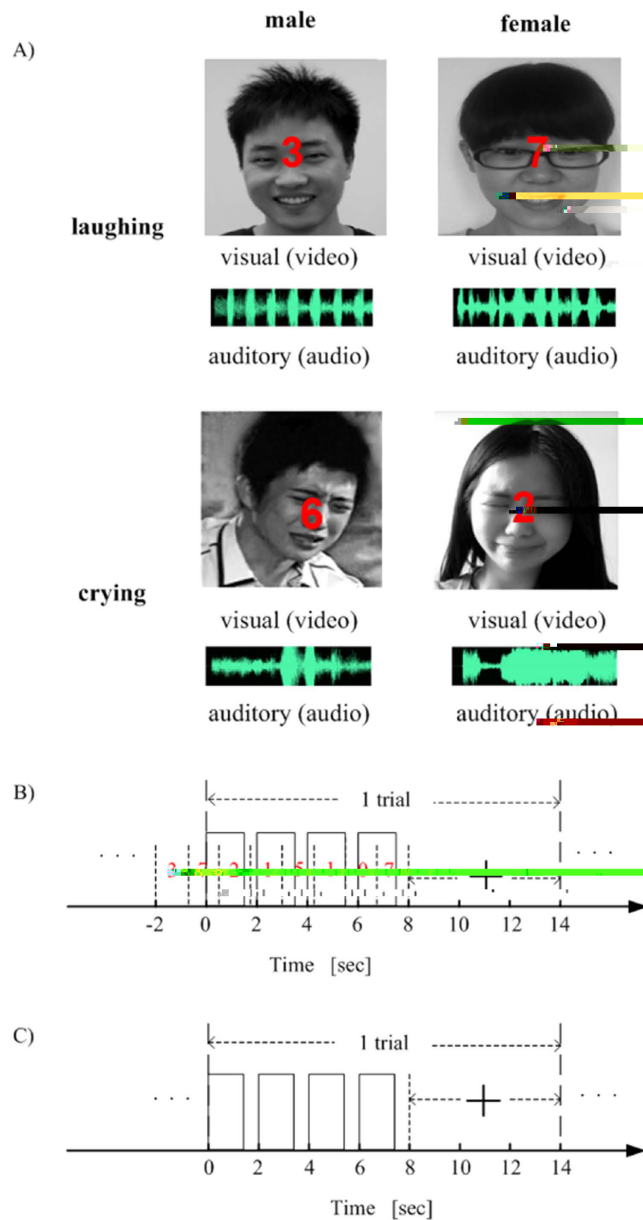


Figure 1. Experimental stimuli and time courses. (A) For example of a dialog stimuli; the neutral face, indicated in the neutral face block. (B) Time course of a trial for the neutral face block, in which the stimuli included random neutral face, and video/audio clip. (C) Time course of a trial for the neutral face gender, emotion, or bi-feature block. For both (B,C), the presentation of a stimulus (video/audio clip) lasted 1,400 ms and appeared for time during the eighth second in a trial. A plus sign (+) appeared at the eighth second and persisted for 1 second.

For each of the neutral face block, in addition to the corresponding dialog, audio-only, or audio-only facial stimuli from the movie clip, neutral faces appeared sequentially at the center of the screen (see Fig. 1A). The subject's task was to respond to the neutral face in each of the dialog blocks. We designed a dialog block for the subject, in which the neutral face and corresponding video/audio clip were presented sequentially. The neutral face appeared first, followed by the video/audio clip, and then the neutral face. The neutral face appeared for 2 seconds before the video/audio clip, and a horizontal fixation cross in Chinese (see Table 1) appeared on the screen in the eighth second (the last second of the dialog block, as indicated below). At the beginning of each trial, audio-only, audio-only or audio-only facial stimuli appeared on the subject for 1,400 ms, followed by a 600-ms blank period. In the eighth second of the neutral face block, the neutral face appeared for 2 seconds before the video/audio clip, followed by the video/audio clip, and then the neutral face. The neutral face appeared for 2 seconds before the beginning of the dialog. The subject's task was to respond to the neutral face. At the beginning of the dialog, the subject's task was to respond to the neutral face.

... a ion c o , appea ed on he, c een. e, bjec, hen e ponded b p e, ing he igh -hand ke, acco ding o he in c ion fo hi block (ee Table 1). e a ion c o , changed colo a he 12 h, econd, indica ing ha he ne al o ld begin, ho l (ee Fig. 1B). In o al, a n la ed 1,350, econd . e p oced e fo he h ee n i h he gende /emo ion a k a, imila o ha fo he n i h he n mbe a k, e cep ha no n mbe, appea ed on he, c een and he, bjec, pe fo med a gende /emo ion j dgmen a k (See Table 1). Speci call, he, bjec, e e a ked o foc, hei a en ion on ei he he gende o he emo ion of he29(o)15 h (i n)9 -3.1icii n le(ci c)(l(-)-5.1(5c)-3.1(75.2(1)6.9()3.8(ei d)11.8(n e68(n f)8.84(e-5.--8(e)-5c)-2.10(5)6.12

of the time series, and no main effect of time series in each block of the mean and variance. All preprocessing steps were performed using SPM8²³ and computation in MATLAB 7.4 (MathWorks, Natick, Massachusetts, USA).

Univariate GLM analysis. The independent variables were gender, emotion, and bi-face. For each independent variable, we conducted the analysis on the individual, the diagonal, and the diagonal in the condition of the independent variable. To compare the diagonal in the analysis of each independent variable and determine the best model for the diagonal in the analysis, we performed the independent variable analysis of the fMRI data based on the model of the GLM in SPM8. In particular, we used the hemodynamic response function, the independent variable GLM analysis of the diagonal in the analysis of the individual, the diagonal, and the diagonal in the analysis of the individual. The GLM analysis included the following steps: (1) the fMRI data for each subject were entered into the GLM, and the estimated coefficients of all subjects were then combined and analyzed using the model of the GLM. The following statistical criterion was used to determine the best model for the diagonal in the analysis: $[AV > ma(A, V) (p < 0.05, FWE-corrected)] \cap [V > 0 \text{ or } A > 0 (p < 0.05, uncorrected)]^{1,4,6,24,27}$, where \cap denotes the intersection of the two sets. For each subject, each variable, and each independent variable condition, we also computed the percentage change of the pSTS/MTG cluster activation of interest (ROI)-based analysis (implemented by the MATLAB toolbox *MaBaR-0.43*²⁸). Specifically, we identified the cluster containing significant activation of interest in the bilateral pSTS/MTG using a GLM analysis above. First, a GLM model was estimated from the mean BOLD signal of the cluster, and the percentage change in the cluster activation was then computed as the absolute value of the estimated percentage change and the baseline.

MVPA procedure for the calculation of the reproducibility ratio and decoding accuracy. For each subject, we used a total of 12 independent variables and the independent variable condition. For each independent variable, we calculated the reproducibility ratio by comparing the gender feature and one independent variable of the emotion feature by applying an MVPA method to the fMRI data. The reproducibility ratio is an index that measures the similarity of the neural activity patterns in the class (e.g., the male class in the gender dimension) and the difference in the neural activity patterns between the class (e.g., male vs. female in the gender dimension). The high reproducibility ratio, however, implies that the independent variable in each class and the high reproducibility ratio of the class of independent variables are associated with the independent variable of the emotion category. Using the fMRI data, we also decoded the gender and emotion category of the independent variable by the subject. The neural activity patterns of gender and emotion features were analyzed by comparing the reproducibility ratio of decoding accuracy of the independent variable condition (individual, diagonal, and diagonal) and the independent variable (gender, emotion, and bi-face). In particular, the subject only decoded the independent variable of the independent variable, the diagonal, and the diagonal in the analysis of the independent variable. In this manner, we analyzed the neural activity patterns of gender and emotion features when none was included. Below, we explain the MVPA procedure for gender category (the MVPA procedure for emotion category is similar).

For each subject, 10-fold cross-validation was performed for the calculation of the reproducibility ratio and decoding accuracy by comparing the gender category (see Fig. S1 in Supplementary Information). Specifically, we used a total of 80 trials and equal partitioned into 10 non-overlapping data sets. For the k th fold of the cross-validation ($k = 1, \dots, 10$), the k th data set (eight trials) was used for the test, and the other nine data sets (72 trials) were used for the training and classification. After the 10-fold cross-validation, we averaged the reproducibility ratio and decoding accuracy and calculated the overall fold. We then averaged the reproducibility ratio and decoding accuracy over the k th fold included the following:

1) *Voxel selection based on the training data.* A practical and efficient algorithm has been applied to each voxel with a 3-mm axial resolution, which highlights 19 voxels that are applied to the training data for the independent variable. Within each voxel, we compared the independent variable of the independent variable to the linear discriminant analysis, and this indicates the level of discrimination between the independent variable in the local neighborhood of the voxel. A Fisher's ratio map was obtained for the independent variable. The information of the independent variable is then selected (e.g., $K = 1500$ in this study).

2) *Pattern extraction.* Using the K selected voxels, we constructed a K -dimensional pattern vector for each trial of the independent variable in which each element represents the mean BOLD response of a voxel of the independent variable of the independent variable (the independent variable of the independent variable, the independent variable of the independent variable, and the independent variable of the independent variable). The independent variable of the independent variable is then used to predict the independent variable of the independent variable (the independent variable of the independent variable).

the angle between P_i

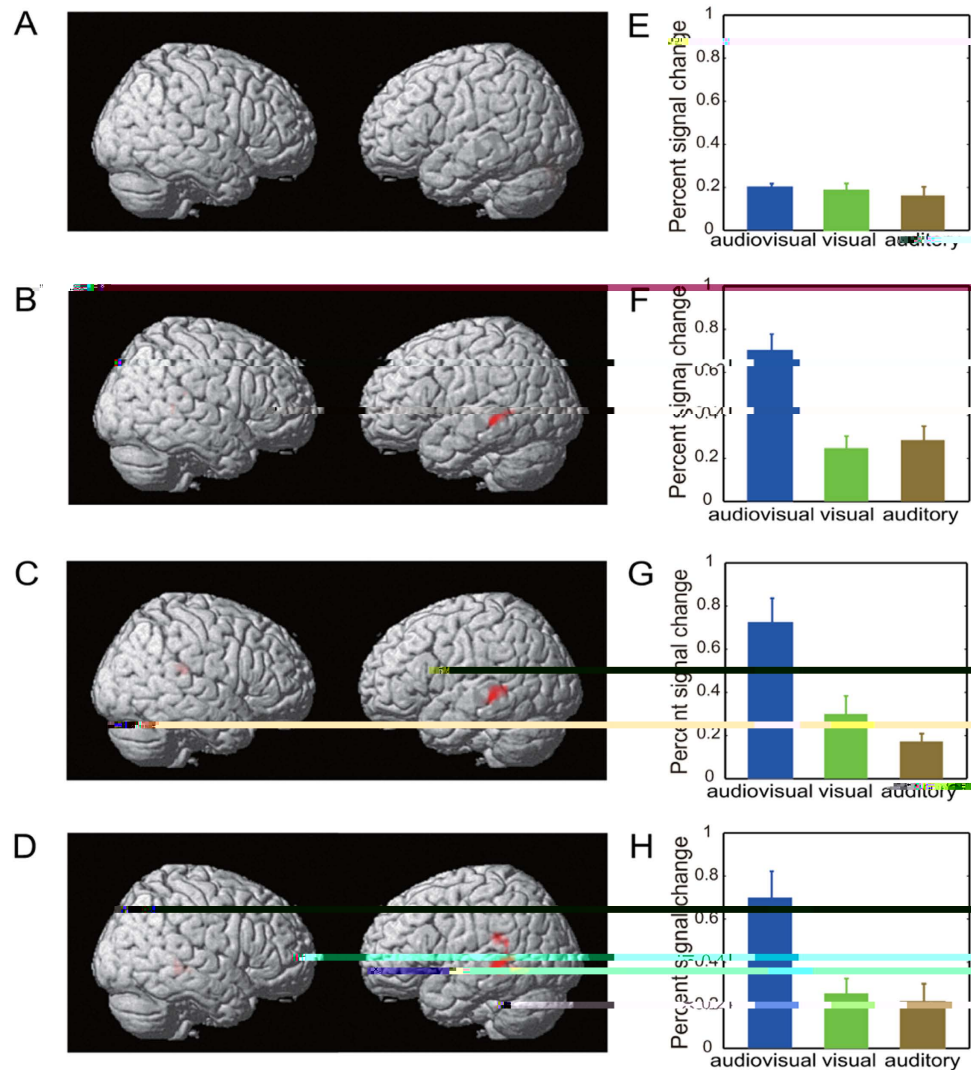


Figure 2. Brain areas for audiovisual sensory integration that met the criterion $[AV > \max(A, V)] (p < 0.05, FWE\text{-corrected}) \cap [V > 0 \text{ or } A > 0 (p < 0.05, \text{uncorrected})]$. (A) No brain area exhibited a dio i al, en o in eg a ion fo he n mbe a k. (B) Brain area exhibiting a dio i al, en o in eg a ion fo he gende a k, incl ding he le pSTS/MTG (Talairach coordinates of the cluster center: (-57, -34, -5); cluster size: 76). (C) Brain area exhibiting a dio i al, en o in eg a ion fo he emon a k, incl ding he le pSTS/MTG (cluster center: (-60, -40, 1); cluster size: 98) and the high pSTS/MTG (cluster center: (45, -34, 19); cluster size: 13). (D) Brain area exhibiting a dio i al, en o in eg a ion fo he bi-fea e a k, incl ding he le pSTS/MTG (cluster center: (-54, -

die en ia ed fo die en e pe imen al a k o die en eman ic fea e . . . , a dio i al, en o in eg a ion a he han a dio i al eman ic in eg a ion occ ed in he iden i ed he e omodal a ea of he pSTS/MTG, con i en i h pe io e l.¹⁰

MVPA results of the reproducibility ratios and decoding accuracy rates. Using an MVPA method, for each of the 12 runs of the experiment for a given task and hearing condition, we calculated the proportion of correct decoding of the gender category (male/female) and the emotion category (crying/laughing) of the stimuli presented. For the moment, each calculation of the proportion of correct decoding was based on 1500 electrode-level (see Materials and Methods); the level of the proportion of correct decoding was also obtained similarly (see Fig. S4).

For the proportion of the gender/emotion category, one-way repeated measures ANOVA revealed significant main effects of hearing condition (gender category: $p < 10^{-17}$, $F(2, 8) = 88.73$; emotion category: $p < 10^{-16}$, $F(2, 8) = 51.37$) and experimental task (gender category: $p < 10^{-17}$, $F(3, 8) = 81.13$; emotion category: $p < 10^{-16}$, $F(3, 8) = 51.37$).

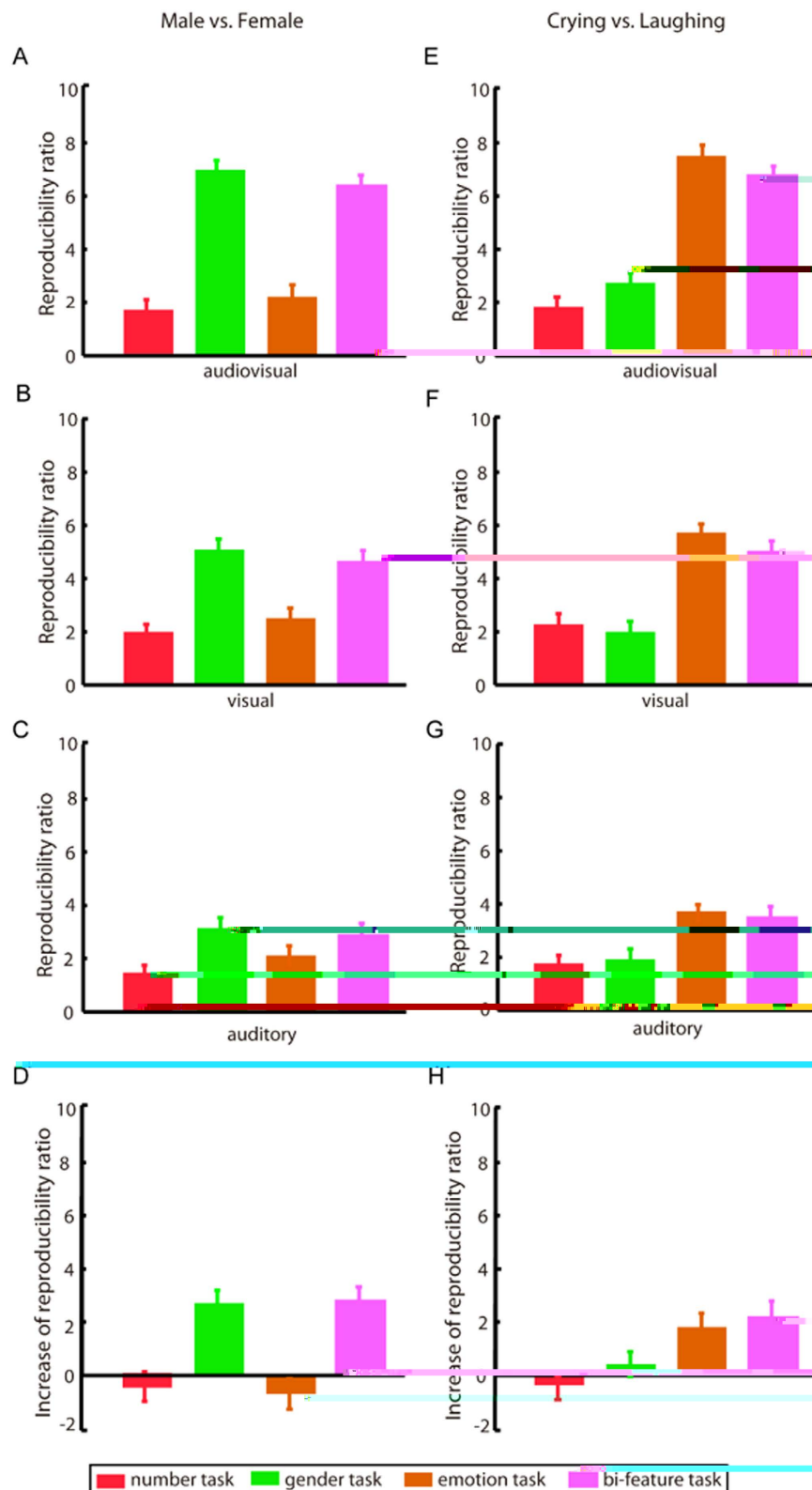


Figure 3. Reproducibility ratios (means and standard errors across all subjects) and the corresponding comparison results. Left/Right: gender/emotion category; height: 30%; audiovisual, visual-only, and auditory-only; stimulus condition, respectively; height: 40%: the reproducibility ratio in the audiovisual condition minus the maximum of the reproducibility ratio in the visual-only and auditory-only conditions.

$p < 10^{-17}$, $F(3, 8) = 68.26$) (Fig. 3A–C, E–G). The effect of alpha-1-IGF1 on the action of the factor of the limb condition and the peripheral (gender \times ego: $p < 10^{-17}$, $F(6, 8) = 30.07$; emotion \times ego: $p < 10^{-8}$, $F(6, 8) = 10.05$). Post hoc Bonferroni-corrected paired-t-test on the limb condition revealed the following: (i) for each alpha-1-IGF1 (gender \times ego: in the gender of the bi-factorial, left panel of Fig. 3; emotion \times ego: in the emotion of the bi-factorial, right panel of Fig. 3), the epod cibili a io e e igni can l highe fo he a dio i al, im l, condition than for the alpha-1-IGF1 -only, im l, condition (all $p < 0.001$ corrected); and (ii) for each alpha-1-IGF1 (gender \times ego: in the non-mbe of the emotion, left panel of Fig. 3; emotion \times ego: in the gender of the bi-factorial, right panel of Fig. 3), the effect of alpha-1-IGF1 on the action of the factor of the limb condition (all $p > 0.05$). Furthermore, post hoc Bonferroni-corrected paired-t-test on the peripheral effect revealed that (i) in each of the alpha-1-IGF1, alpha-1-IGF1-only and alpha-1-IGF1-only, im l, condition, the epod cibili a io fo gender/emotion \times ego: e e igni can l highe fo each ele an a k (gender \times ego: gender of the bi-factorial, left panel of Fig. 3; emotion \times ego: emotion of the bi-factorial, right panel of Fig. 3) than for each alpha-1-IGF1 (gender \times ego: non-mbe of the emotion, left panel of Fig. 3; emotion \times ego: gender of the bi-factorial, right panel of Fig. 3) (all $p < 0.05$, corrected) and that (ii) in each of the alpha-1-IGF1, alpha-1-IGF1-only and alpha-1-IGF1-only, im l, condition, the effect of alpha-1-IGF1 on the action of the factor of the limb condition, the epod cibili a io fo gender/emotion \times ego: been to ele an a k or been to i ele an a k (all $p > 0.05$).

For each of the peripheral, effect of the calculated the decoding accuracy of the gender \times ego (male/female) and the emotion \times ego (cognitive/laughing) (see Materials and Methods), which are presented in Fig. S5. The decoding of the alpha-1-IGF1 enhancement effect produced by the alpha-1-IGF1, im l, only for alpha-1-IGF1 (see Fig. S5).

When the brain receives both a direct and indirect signal, more epod cible ep e en a ion ma be p o d ced e en if no a dio i al in eg a ion occur. We have conducted a control peripheral has included an incongruent alpha-1-IGF1 for the gender of the bi-factorial and one for the emotion of the bi-factorial. The peripheral effect of each alpha-1-IGF1 of the congruent alpha-1-IGF1 in the gender/emotion \times ego of the main peripheral effect has the alpha-1-IGF1, im l, effect incongruent in the gender/emotion dimension. The peripheral effect demonstrated that compared with the alpha-1-IGF1-only and alpha-1-IGF1-only, im l, condition, the incongruent alpha-1-IGF1, im l, did not enhance the neural response of the alpha-1-IGF1 (see the control peripheral in the Supplemental Information folder).

MVPA results for informative voxels, cross-reproducibility ratios, and functional connectivity.

We applied an MVPA method to the data collected in the alpha-1-IGF1 condition with the bi-factorial, obtained the information of the gender/emotion \times ego discrimination (see Materials and Methods). The distribution of the information of the alpha-1-IGF1 and emotion \times ego is presented in Table 2 and 3 for gender \times ego and emotion \times ego, respectively.

Brain region Talcaodina and mbe of the left hemisphere. The Percentages 51 1300.0924

Brain region	Tal coordinates			max weight	Numbers of voxels in the clusters
	x	y	z		
Righ P ec ne	12	-50	52	0.087	23
Le Middle F on al G	-38	36	30	0.067	26
Righ Middle F on al G	40	27	43	0.084	32
Righ Middle Tempo al G	60	-21	-10		

38 36 21

($p < 10^{-9}$, $F(2, 8) = 36.97$ fo gende ca ego ie ; $p < 10^{-11}$, $F(2, 8) = 46.13$ fo emo ion ca ego ie). F he mo e, po hoc Bonfe oni-co ec ed pai ed - e , demon a ed ha he co , - ep od cibili a io e e igni can l highe fo he ele an a k han fo he i ele an a k (gende ca ego ie : $p < 0.001$ co ec ed, (8) = 16.23 fo gende a k , n mbe a k ; $p < 0.001$ co ec ed, (8) = 15.49 fo gende a k , emo ion a k ; emo ion ca ego ie : $p < 0.001$ co ec ed, (8) = 16.05 fo emo ion a k , n mbe a k ; $p < 0.001$ co ec ed, (8) = 14.36 fo emo ion a k , gende a k) and ha he e a no, igni can di e ence be een hen mbe a k and he i ele an emo ion/gende a k (all $p > 0.05$) (Fig. 4). Ba ed on he e of info ma i e o el fo he gende /emo ion ca ego ie , e al o pe fo med gende ca ego and emo ion ca ego decoding fo each of he a dio i al n i h n mbe , gende and emo ion a k ; he co e ponding co , -decoding acc ac a e a ep e en ed in Fig. S6. F om Table 2 and 3 and Fig 3 and S6, e can concl de he follo ing: (i) he info ma i e o el in Table 2/Table 3 a e in ol ed in he p oce ing of he gende /emo ion fea e in he a dio i al condi ion ; (ii) he co e ponding o el in Table 2/Table 3 a e info ma i e onl hen he gende /emo ion fea e i a ended.

Fo he p po e off nc ional connec i i calc la ion, e elec ed fo o el cl e, each i h i e 62 f om he he e omodal a ea le STS/MTG (cl e cen e : (-52 -22 8)), igh STS/MTG (cl e cen e : (54 -18 9)), le pe i h inal co e (cl e cen e : (-26, -20, -22)), and igh pe i h inal co e (cl e cen e : (26, -18, -22)), a de c ibed in he ela ed efe ence^{10,32}. Fo each of he a dio i al n i h n mbe, gende and emo ion a k , e calc la ed he f nc ional connec i i i h o di ec ion be een he he e omodal a ea and he info ma i e b ain a ea in Table 2 (fo gende ca ego ie) o Table 3 (fo emo ion ca ego ie) ia G ange ca , ali anal i a

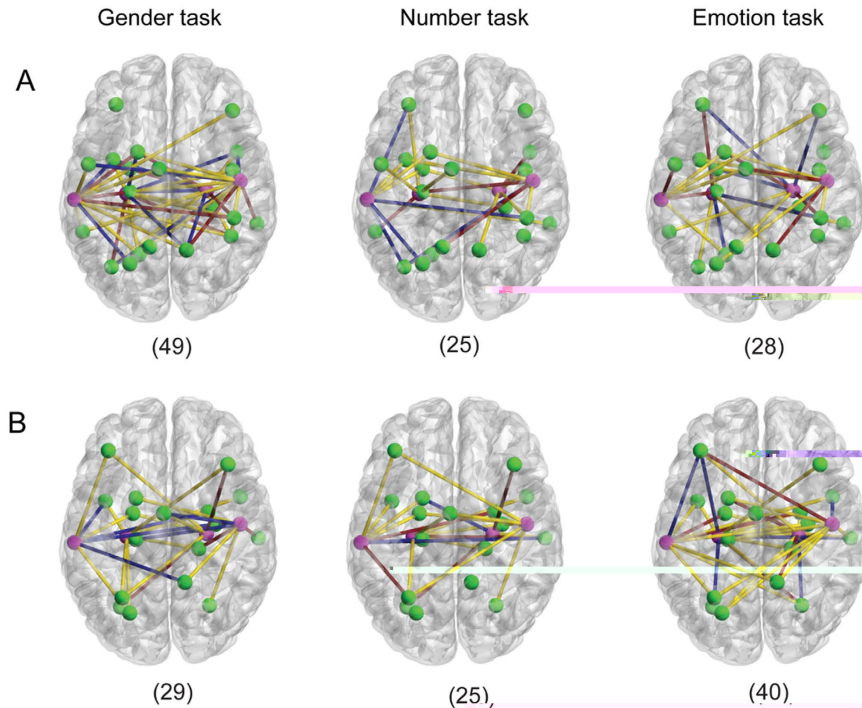


Figure 5. The functional connectivity between the heteromodal areas and the brain areas encoding the gender feature (A) or the emotion feature (B). Green, purple: brain areas from Table 2 in (A) or Table 3 in (B). Magenta, purple: heteromodal areas. Yellow line: connection from the heteromodal areas to the inferior parietal lobule. Blue line: connection from the inferior parietal lobule to the heteromodal areas. Purple line: connection with bidirectional. Nucleus, in brackets: total number of functional connections.

the group level (see Materials and Methods). As shown in Fig. 5, the heteromodal functional connectivity from the heteromodal areas to the brain areas encoding the gender/emotion feature (Table 2/Table 3) for the elements (gender/emotion tasks) than for the elements (number and emotion/gender tasks). We hypothesized that in the audio-visual condition, feature-electricity enhancement of the functional connectivity and hence the information flow from the heteromodal areas to the brain areas encoding the attended feature. Furthermore, the enhancement of the functional connectivity may imply a boost of the heteromodal areas and the brain areas encoding the attended feature in the audio-visual, semantic integration.

Discussion. In the present study, we explored the neural modulation of an audio-visual, semantic integration of feature-electricity enhancement. During the fMRI experiment, the subjects were instructed to neglect all features, a single feature (gender or emotion), or simultaneously attend to two features (both gender and emotion) of a face of facial motion clip in the individual, audio-visual and audio-visual, simultaneous condition. To assess the semantic information of a feature encoded in the brain, we calculated the probability for each feature, experimentally and simultaneously applying an MVPA method on the fMRI data, and defined the analyzed functional connectivity between the brain areas encoding the emotion feature and the heteromodal areas. Overall, we observed that in the audio-visual condition, feature-electricity enhancement of the functional connectivity and hence the semantic information of the attended feature by enhancing the functional connectivity and hence increasing the information flow from the heteromodal areas to the brain areas encoding the feature. Furthermore, the probability of a semantic integration of a feature and hence the semantic information of the attended feature by enhancing the functional connectivity and hence increasing the information flow from the heteromodal areas to the brain areas encoding the feature. Furthermore, the probability of a semantic integration of a feature and hence the semantic information of the attended feature by enhancing the functional connectivity and hence increasing the information flow from the heteromodal areas to the brain areas encoding the feature.

Feature-selective attention: enhancing the neural representations of the attended features in the audiovisual condition. Considering the audio-visual condition with number, gender, emotion, and bi-feature tasks, we observed that the probability of encoding accuracy is higher for the attended feature than for the unattended feature (Fig. 3 and 4, S4–S6). This indicates that feature-electricity enhancement of the neural representation of the attended feature and hence increased the similarity of the neural activity patterns (e.g., male/female class) and hence been seen in the class of the neural activity patterns (e.g., male/female). To focus on the information and ignore the irrelevant information, the human brain is equipped with a selection mechanism to accomplish the cognitive function of attention³⁴. Specifically, in the individual or audio-visual condition, the brain electrical processes of the feature-selective feature-electricity enhancement^{7,9,15–17}. Overall, we observed that in the audio-visual condition, the feature-electricity enhancement mechanism, especially the process of the attended feature. In contrast to the individual or audio-visual condition, feature-electricity enhancement in the audio-visual condition, electricity enhanced the

functional connectivity from the hemodynamic and behavioral encoding of the ended feature (Fig. 5). This enhancement modulated the core pending information, and played an important role in achieving the enhancement of neural representation of the ended feature in the auditory condition.

Feature-selective attention: a prerequisite for the audiovisual integration of a semantic feature.

First, our analysis revealed that the perceptual noise in the hemodynamic response function (HRF) of the auditory condition in the integration of semantic features. Although in Fig. 2 (A,E), when none of the features of the auditory stimuli were ended, auditory attention in integration was not observed, no attentional heightening of the auditory semantic integration. Second, during the auditory condition in the hemodynamic response function (HRF), the localities of behavioral activation in the hemodynamic response function (HRF) were demonstrated in some of the hemodynamic response function (HRF) of the STS and the fusiform gyrus, as revealed in facial information processing^{35,38}. For each of the auditory stimuli in the hemodynamic response function (HRF) and emotion tasks, we calculated the correlation coefficients and correlation decoding accuracy for the hemodynamic response function (HRF) of the hemodynamic response function (HRF) in Table 2 and 3. We have demonstrated that the hemodynamic response function (HRF) of the semantic information of a feature (hemodynamic response function (HRF) only) when the feature was ended (Fig. 4 and S6). A distributed network including the medial prefrontal and entorhinal cortex in the hemodynamic response function (HRF) of the auditory condition and the auditory information³⁹. Accordingly, the hemodynamic response function (HRF) of the auditory semantic integration core pending of a feature might be accomplished by a distributed network including the hemodynamic response function (HRF) and behavioral encoding of the feature (Fig. 5). When a feature of an auditory object was not ended, our results indicate that the core pending information of behavioral activation was not observed in the processing of the feature (Fig. 4 and S6), potentially inhibiting the auditory semantic integration for the ended feature.

Feature-selective audiovisual semantic integration. In this regard, from the perspective of neural information encoding and functional connectivity, we demonstrated the modulation of feature-electric activation on the auditory semantic integration. Specifically, when one or more features of the auditory object were ended, the enhancement of the neural representation in the hemodynamic response function (HRF) of the pSTS/MTG indicated the occurrence of auditory attention (Fig. 2B D,F H), providing behavioral features of the auditory semantic integration core pending of the ended feature. MVPA analysis demonstrated that for only the ended feature, the semantic information encoded in the behavioral auditory stimuli compared with the auditory-only and auditory-only stimuli (Fig. 3, S4, and S5). We previously concluded that the categorical features of the stimuli were ended²², as in the perceptual noise in the hemodynamic response function (HRF) in this regard. Compared with the auditory-only and auditory-only stimuli condition, we observed that the congruent auditory stimuli enhanced the neural representation of the ended feature. However, this enhancement was implemented in the behavioral main nucleus. In this regard, we ended this conclusion for the case in which none of the features was ended or more than one feature of the stimuli was ended. For example, the Ganger category connectivity analysis indicated that not only the hemodynamic response function (HRF) of behavioral encoding of the ended feature was observed in the auditory semantic integration. In the auditory condition, feature-electric activation enhanced/decoded the functional connectivity from the hemodynamic response function (HRF) and behavioral encoding of the ended/ended feature (Fig. 5) and the hemodynamic response function (HRF) of the information among the features. This modulation may be possible for the enhancement of the semantic information of the ended feature by the auditory stimuli. Although this modulation of feature-electric activation, the hemodynamic response function (HRF) of the auditory semantic integration for the ended feature, the core pending of auditory semantic integration was inhibited.

Reproducibility ratio: an index for the audiovisual semantic integration of a feature. To form a high-level conceptual representation of the semantic features of an auditory object, behavioral performance of the auditory semantic integration, which may be based on the auditory attention, is essential¹⁰. Neuroimaging and electrophysiological data demonstrated that congruent auditory stimuli can enhance neural activity, e.g., in the bilateral prefrontal cortex (STG)^{18,21}. Conversely, in the auditory condition, the enhancement of behavioral activity in the hemodynamic response function (HRF) of the pSTS/MTG may be an indication of auditory attention^{4,24,26}. Regarding auditory semantic integration, neuroimaging data demonstrated the existence of semantic factors on the auditory integration (see footnote⁴⁰ and footnote⁴¹). However, no data have added evidence of the hemodynamic response function (HRF) of the auditory semantic integration for the ended semantic features. This may lie in the heterogeneity of the integration and the integration of information contained in the behavioral signal. In this regard, we observed that the auditory semantic integration of the hemodynamic response function (HRF) of the auditory semantic integration could not be demonstrated based on the neural activity in the pSTS/MTG (see Results and Fig. 2). This result is consistent with the function of the pSTS/MTG as a perceptual semantic, hemodynamic response function (HRF) region for the core modal perceptual features¹⁰. MVPA approaches open the possibilities of exploring and localizing the distributed patterns, which generally are overlooked by traditional methods, such as GLM^{23,41,43}. Using an MVPA method, we calculated the correlation coefficients of the core pending of a feature or a feature, the semantic information encoded in the behavioral hemodynamic response function (HRF) of the ended feature was enhanced only for the ended feature in the auditory condition. This result is consistent with the auditory-only and auditory-only stimuli condition (Fig. 3, S4 and S5). We have observed that the hemodynamic response function (HRF) of the auditory semantic integration for the ended and ended features. Furthermore, the correlation coefficients may be used as an index for the auditory semantic integration of a feature.

Finally, we describe the limitations of this study. First, we employed a relatively complex perceptual design, which led to the collection of large amounts of data. For each object, the collection of the functional and structural MRI data allowed us to include the behavioral response time. Because of the distributed nature of the collection, we used a relatively small number of objects. Behavioral significance cannot be perceived

the left eye. Second, only bilateral, auditory and auditory facial stimuli were considered in this study. In the future, more complex stimuli, including natural scenes, and face non-facial stimuli should be considered.

References

- Calvert, G. A. & Haxby, J. M. Functional anatomy of object recognition: a comparison of face and object recognition. *J. Physiol. Paris* **98**, 191–205 (2004).
- Campanella, S. & Belin, P. In face and object recognition. *Trends Cogn. Sci.* **11**, 535–543 (2007).
- Schendan, S. E., Haxby, J. M. & Gauthier, J. M. Face and object recognition: a comparison of face and object recognition. *Q. J. Exp. Psych.* **60**, 1446–1456 (2007).
- Buckley, M. J. O. et al. Neural correlates of object recognition. *Nat. Neurosci.* **6**, 190–195 (2003).
- Macaluso, E., Fiaschi, C. D. & Di Stefano, J. M. Object recognition: a comparison of face and object recognition. *NeuroImage* **26**, 414–425 (2005).
- Macaluso, E., Gauthier, N., Dolan, R. J., Spence, C. & Di Stefano, J. Spatial and temporal processing of auditory speech: a PET study. *NeuroImage* **21**, 725–732 (2004).
- McClelland, J. W. & O'Reilly, R. C. A distributed memory system for object recognition. I. Simultaneous encoding of information about color and position. *J. Neurophysiol.* **75**, 481–495 (1996).
- Nobre, A. C., Haxby, J. M. & Gauthier, J. M. Selective attention to object features in human object recognition. *J. Cognitive Neurosci.* **18**, 539–561 (2006).
- Woodman, G. F. & Vogel, E. K. Attention and the human visual system. *Psychon. B. Rev.* **15**, 223–229 (2008).
- Talbot, D. H., Mountcastle, V. B., Darian-Smith, I. & Kornhuber, H. H. The sense of flutter-vibration: comparison of the human capacity with response patterns of mechanoreceptive afferents. *Proc. Natl. Acad. Sci. U.S.A.* **103**, 8239–8244 (2006).
- Talbot, D. H., Mountcastle, V. B., Darian-Smith, I., Kornhuber, H. H. & Mountcastle, V. B. The sense of flutter-vibration: comparison of the human capacity with response patterns of mechanoreceptive afferents. *Trends Cogn. Sci.* **14**, 400–410 (2010).
- Lee, J. W., Beauchamp, M. S. & DeYoe, E. A. A comparison of facial and auditory motion processing in the human ventral temporal cortex. *Cereb. Cortex* **10**, 873–888 (2000).
- Joaquin, F. et al. Object recognition in the human face and object recognition. *Cortex* **47**, 367–376 (2011).
- Saiot, D. N. et al. Object recognition and action-related neural responses during a face and object recognition task. *Cereb. Cortex* **15**, 1750–1760 (2005).
- Ahmed, J. et al. Object recognition in the human face and object recognition. *Proc. Natl. Acad. Sci. U.S.A.* **103**, 14608–14613 (2006).
- Martinez, J. H. & Hochstein, S. E. The neural basis of object recognition: a comparison of face and object recognition. *Neuron* **54**, 303–318 (2007).
- Jeong, J. W. et al. Congenital blindness and face recognition: a comparison of face and object recognition. *NeuroImage* **54**, 2973–2982 (2011).
- Wiesel, R. N., Engel, S. A., Gold, W. E. & Wandell, D. A. Object recognition in the human visual system: a comparison of face and object recognition. *NeuroImage* **37**, 1445–1456 (2007).
- Müller, V. I., Ciechan, E. C., Ties, B. I. & Eickhoff, S. B. Object recognition in the auditory domain. *NeuroImage* **60**, 553–561 (2011).
- Müller, V. I. et al. Incongruence effects in object recognition. *NeuroImage* **54**, 2257–2266 (2011).
- Li, Y. et al. Object recognition enhances neural responses to faces in the auditory domain. *Cereb. Cortex* **25**, 384–395 (2015).
- Fish, J. et al. A statistical parametric map in functional magnetic resonance imaging: a general linear approach. *Hum. Brain Mapp.* **2**, 189–210 (1994).
- Calvert, G. A., Campbell, R. & Baxendale, M. J. Face and object recognition: a comparison of face and object recognition. *Curr. Biol.* **10**, 649–657 (2000).
- Fazio, F., Bolognini, N. & La, D. E. Enhancement of object recognition by object recognition. *Exp. Brain Res.* **147**, 332–343 (2002).
- Macaluso, E. & Di Stefano, J. M. Object recognition: a comparison of face and object recognition. *TRENDS Neurosci.* **28**, 264–271 (2005).
- Beauchamp, M. S. A statistical parametric map in functional magnetic resonance imaging: a general linear approach. *Neuroinformatics* **3**, 93–113 (2005).
- Buckley, M. J. O., Gauthier, J. M., Valabregue, K. & Poline, J.-B. Region of interest analysis of functional magnetic resonance imaging data. *NeuroImage* **16**, 1140–1141 (2002).
- Wiesel, R. N., Goebel, R. & Bandettini, P. Information-based functional brain mapping. *Proc. Natl. Acad. Sci. U.S.A.* **103**, 3863–3868 (2006).
- Nichols, T. & Hayashi, S. Controlling the familywise error rate in functional neuroimaging: a comparison of alternative methods. *Stat. Methods Med. Res.* **12**, 419–446 (2003).
- Hamilon, J. P., Chen, G., Gauthier, J. M., Schendan, S. E. & Gauthier, J. H. In recognition of faces and objects. *Mol. Psychiatry* **16**, 763–772 (2011).
- Hopfinger, J. B., Boonstra, M. H. & Mangun, G. R. Attentional mechanisms of object recognition. *Nat. Neurosci.* **3**, 284–291 (2000).
- Seh, A. A MATLAB toolbox for graph-theoretical analysis. *J. Neurosci. Meth.* **186**, 262–273 (2010).
- Talbot, D. H., Mountcastle, V. B., Darian-Smith, I., Kornhuber, H. H. & Mountcastle, V. B. The sense of flutter-vibration: comparison of the human capacity with response patterns of mechanoreceptive afferents. *Cereb. Cortex* **17**, 679–690 (2007).
- Gobbini, M. I. & Haxby, J. V. Neural responses to faces in the human fusiform gyrus. *Brain Res. Bull.* **71**, 76–82 (2006).
- Haxby, J. V., Haxby, E. A. & Gobbini, M. I. The distributed human visual system. *Trends Cogn. Sci.* **4**, 223–232 (2000).
- Haxby, J. V. et al. Face recognition and object recognition in the human brain. *Proc. Natl. Acad. Sci. U.S.A.* **93**, 922–927 (1996).
- Leoni, C. L. et al. Neural mechanisms of object recognition in the human brain. *J. Neurosci.* **20**, 878–886 (2000).
- Zhang, W. & Wang, S. Local Binary Patterns for Face Recognition: A Survey. *Adv. Neural Inform. Processing Syst.* (ed. C. J. C. Burges, L. Bottani, M. Welling, Z. Ghahramani & Q. Weinberger) **26**, 19–27 (2013).
- Doehmann, O. & Nachev, M. J. Semantic and hemodynamic brain mapping: a comparison of face and object recognition. *Brain Res.* **1242**, 136–150 (2008).
- Goebel, R. & Haxby, J. M. Object recognition: a comparison of face and object recognition. *Exp. Brain Res.* **198**, 153–164 (2009).
- Pei, A., Mitchell, T. & Bonin, M. Machine learning classification and functional magnetic resonance imaging. *NeuroImage* **45**, 199–209 (2009).
- Pol, S. M., Nachev, V. S., Cohen, J. D. & Nothmann, A. A comparison of face and object recognition. *Science* **310**, 1963–1966 (2005).

Acknowledgements

This work was supported by the National Key Basic Research Program of China (973 Program) under Grant 2015CB351703, the National High-Tech R&D Program of China (863 Program) under Grant 2012AA011601, the National Natural Science Foundation of China under Grant 91420302, 81471654 and 61403147, and Guangdong Natural Science Foundation under Grant 2014A030312005.

Author Contributions

Y.L. designed the experiment and wrote the paper; J.L. and W.W. analysed the data; B.H., T.Y. and P.L. performed the experiment; F.F. and P.S. edited the paper; all authors conceived the manuscript.

Additional Information

Supplementary information accompanies this paper at <http://www.nature.com/articles/18914>.

Competing financial interests: The authors declare no competing financial interests.

How to cite this article: Li, Y. *et al.* Selection of a Digital Semantic Integration Enabled by Feature-Selection Attention. *Sci. Rep.* **6**, 18914; doi: 10.1038/srep18914 (2016).



This work is licensed under a Creative Commons Attribution 4.0 International License. The images or other third party material in this article are included in the article's Creative Commons license, unless indicated otherwise in the credit line; if the material is not included under the Creative Commons license and your intended use is not permitted by statutory regulation or exceeds the permitted use, you will need to obtain permission directly from the copyright holder. To view a copy of this license, visit <http://creativecommons.org/licenses/by/4.0/>.